

PACS numbers: 42.55. Lt
DOI: 10.1070/QE2008v038n04ABEH013628

Analytic study of the temperature profile in a copper bromide laser

I.P. Iliev, S.G. Gocheva-Ilieva, N.V. Sabotinov

***Abstract*. Based on the two-dimensional heat conduction equation solved under boundary conditions of the third and fourth kind, a new approach is proposed for determining the gas temperature in the cross section of a copper bromide laser. Temperature profiles in the cases of the natural and forced convection are obtained taking into account the basic laser parameters such as the laser design, the input electric power, etc. In particular, computer simulations for the case of forced convection are performed in order to increase the input electric power at a fixed maximum discharge temperature.**

Keywords: *copper bromide laser, temperature profile, model.*

1. Introduction

Copper and copper vapour lasers with additives attract the greatest interest among metal vapour lasers because they appear to be the most powerful radiation sources in the visible region. Although considered well known, they continue to be the subject of experimental studies [1, 2]. To improve the laser characteristics and to study the physical processes in the active laser medium, various mathematical models for computer simulation of the kinetic processes in these lasers were developed [3 – 5].

When determining the gas temperature, two main approaches are usually applied – setting the tube wall temperature [3, 4] or fixing the gas temperature in advance, this parameter being constant in the following computer simulations [5]. However, during lasing and in the process of the computer simulations, the gas temperature must be thoroughly controlled, because it is an important thermodynamic characteristic of the active laser medium. It characterises the laser lifetime, the lasing decay time, and the distribution of the neutral atoms in the cross section of the tube. Thermally the lower laser levels are populated, which affects the laser power and the laser beam mode composition. The high temperature can cause thermoionisation instability of the gas discharge. On the other hand, during various computer simulations, it is possible to change the geometrical design, the tube materials and the heat insulation, the input electric power, as well as the laser operating conditions. In this case, the wall temperature remains unknown. The temperature profile set in advance can also be changed. This means that, if the gas temperature is not correctly specified, the obtained results can be unreliable. Special attention is paid to this problem in [6].

The aim of this paper is to develop a new analytic model for obtaining more accurate values of the gas temperature in the cross section of copper bromide vapour lasers. For this purpose, the two-dimensional heat conduction equation is considered, which is subjected to nonlinear boundary conditions of the third and fourth kind instead of the boundary condition of the first kind that is usually applied. At a given air temperature of the surroundings (for instance, $T_0 = 300$ K), due to the heat convection and heat radiation, the proposed approach permits taking into account the heat exchange processes between the outer surface of the tube and its surroundings. The gas temperature profile in the tube and the outside wall temperature are expressed by solving the heat conduction equation and directly depend on the basic input laser parameters – its geometric design, the input electric power, etc. The derived analytical model is used to study the gas temperature variation particularly in the case of forced cooling of the laser tube.

2. Description of the method

We studied a copper bromide vapour laser [7]. The total consumed power is 5000 W, while the output laser power is 120 W. Taking into account the electric power losses in the power supply, the laser tube is fed with power $Q_1 =$ 4800 W, and the laser efficiency is 2.5 %. Research shows [8] that about 15 % of the power Q_1 is lost on the electrodes (10 % on the cathode and 5 % on the anode). In this way, the power $Q = 4080$ W is supplied to the active volume of the laser tube. The geometrical dimensions of the tube are shown in Fig. 1. The laser tube is manufactured from quartz and the active laser volume is covered with extra heat-insulating wadding made of felt – glass, mineral material or zircon dioxide.

In modeling the temperature profile, the following assumptions are made: 1) the temperature profile is determined in the quasi-stationary regime; 2) the gas temperature

I.P. Iliev Department of Physics, Technical University of Plovdiv, 25 Tzanko Djusstabanov St., 4000 Plovdiv, Bulgaria; e-mail: iliev55@abv.bg;
S.G. Gocheva-Ilieva Department of Applied Mathematics and Modelling, Faculty of Mathematics and Informatics, Paisii Hilendarski University of Plovdiv, 24 Tzar Assen St., 4000 Plovdiv, Bulgaria; e-mail: snow@uni-plovdiv.bg, snegocheva@yahoo.com;
N.V. Sabotinov Metal Vapour Lasers Department, Georgi Nadjakov Institute of Solid State Physics, Bulgarian Academy of Sciences, 72 Tzarigradsko Chaussee, 1784 Sofia, Bulgaria;
e-mail: nsabotinov@issp.bas.bg

Received 14 May 2007; revision received 26 December 2007
Kvantovaya Elektronika **38** (4) 338 – 342 (2008)
Translated by M.N. Sapozhnikov

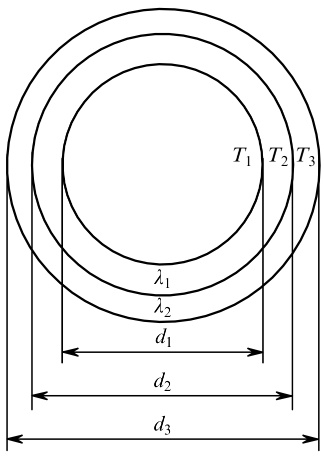

Figure 1. Cross section of the copper bromide laser tube ($d_1 = 60$ mm, $d_2 = 64$ mm, $d_3 = 74$ mm).

does not change substantially between excitation pulses; 3) the power distribution in the active volume is even and the possible contractions of the discharge are not considered; 4) all the input electric power $Q = 4080$ W in the active volume is transformed into heat, while the power given to the tube walls by the discharge emission and the deactivation of the stimulated and charged particles is not considered.

Assumptions 3 and 4 are made due to the lack of reliable enough experimental and analytic research of the temperature profile of copper bromide vapour lasers. For this reason, the obtained temperature profile may differ from the real one, and it is not possible to estimate the errors made in the calculations.

The proposed model can be used for a comparative analysis at the planning stage of the experiment. In the process of computer simulations related to a change in the geometric design, the tube material, the heat insulation, the electrical power and the exploitation conditions, the basic tendencies in changing the temperature profile can be determined.

In this way, there can be specified the most likely parameters, defining the most favorable temperature profile. Thus the quantity of experimental research can be reduced.

The two-dimensional quasi steady-state heat conduction equation in the cross section of the laser tube has the form

$$\mathrm{div}(\lambda_g \, \mathrm{grad} T_g) + q_v = 0, \tag{1}$$

where λ_g is the thermal conductivity of the gas; q_v is the volume density of the internal heat source; and T_g is the temperature in the tube.

Usually, as mentioned above, equation (1) is solved under the boundary condition of the first kind, by specifying the outside surface temperature of the quartz tube T_2. Commonly, the coefficient λ_g is approximated as $\lambda_g = \lambda_0 \times T^m$. In this case, the solution of equation (1) is represented by the expression (see [9])

$$T_g(r) = \left[T_2^{m+1} + \frac{q_v(m+1)}{4\lambda_0}\left(R^2 - r^2\right)\right]^{1/(m+1)}, \tag{2}$$

where R is the tube radius. Solution (2) of equation (1) for the boundary condition of the first kind was used to determine the temperature profile of the copper bromide vapour laser in [10], and also in computer simulations of pure copper vapour lasers in [4]. Up to this point we have failed to find other boundary conditions that can be used to analytically solve equation (1) for copper and copper compound vapour lasers.

To solve equation (1), we use mixed boundary conditions of the third and fourth kind, which, for the cylindrical configuration, have the form [11]:

$$T_1 = T_2 + \frac{q_l \ln(d_2/d_1)}{2\pi\lambda_1}, \; T_2 = T_3 + \frac{q_l \ln(d_3/d_2)}{2\pi\lambda_2}, \tag{3a}$$

$$Q = \alpha F_3 (T_3 - T_0) + F_3 \varepsilon c \left[\left(\frac{T_3}{100} \right)^4 - \left(\frac{T_0}{100} \right)^4 \right]. \tag{3b}$$

Boundary conditions (3a) represent the equation for the continuity of the heat flow at the interface between two media. Here, $q_l = Q/l_a$ is the power per length; $l_a = 2$ m is the active length of the laser [7]; λ_1 and λ_2 are the quartz tube thermal conductivity and thermal insulation coefficients, respectively. Boundary condition (3b) shows the heat exchange between the outer surface of the laser tube and the surroundings. The first term on the right hand side of (3b) evolves from the Newton–Riemann law for heat exchange by convection. The second term represents the Stefan–Boltzmann law for heat exchange by radiation. The value of Q is equal to the electric power $Q = 4080$ W (in accordance with assumption 4); α is the heat transfer coefficient; F_3 is the outer active surface of the tube; ε is the integral emissivity of the material; $c = 5.67$ W m^{-2} K^{-4} is the black body radiation coefficient; and $T_0 = 300$ K is the air temperature. In boundary condition (3b) there are two unknown values – α and T_3. To obtain T_3, we need to evaluate preliminary the heat transfer coefficient α.

2.1 Determination of the heat transfer coefficient α and the gas temperature T_g at natural convection

For all types of convection, the Nusselt criterion has the form [11]:

$$\mathrm{Nu} = \frac{\alpha H}{\lambda}, \tag{4}$$

For free convection, the Grashoff criterion is given by the expression [11]:

$$\mathrm{Gr} = g\beta H^3 \, \frac{T_3 - T_0}{\nu^2}. \tag{5}$$

For the horizontal tubes at natural convection, the two upper criteria can be related by the equality [11]

$$\mathrm{Nu} = 0.46 \mathrm{Gr}^{0.25}, \tag{6}$$

which is valid for $700 < \mathrm{Gr} < 7 \times 10^7$. In the previous expressions (4)–(6), H is a characteristic dimension of the tube (here, $H = d_3$); g is the gravitational acceleration; β is the coefficient of cubical heat expansion of the gas, which for the air is $\beta_{air} = 3.41 \times 10^{-3}$ K^{-1}; ν is the kinematical viscosity $\nu_{air} = 15.7 \times 10^{-6}$ m^2 s^{-1}; λ is the thermal conductivity; $\lambda_{air} = 0.0251$ W m^{-1} K^{-1}. The data is correct for the air temperature 300 K [11].

Taking into consideration (4)–(6) we have:

$$\alpha = 0.46\lambda_{\rm air}\left[g\beta_{\rm air}d_3^3\,\frac{T_3 - T_0}{\nu_{\rm air}^2}\right]^{0.25}\frac{1}{d_3}. \tag{7}$$

Boundary condition (3b), which is represented with respect to the power per unit length, has the form:

$$q_l = 0.46\pi\lambda_{\rm air}\left[g\beta_{\rm air}d_3^3\,\frac{T_3 - T_0}{\nu_{\rm air}^2}\right]^{0.25}(T_3 - T_0) + \pi d_3\varepsilon c\left[\left(\frac{T_3}{100}\right)^4 - \left(\frac{T_0}{100}\right)^4\right]. \tag{8}$$

Now, the outside temperature T_3 can be calculated by solving this nonlinear equation. It is not difficult to establish that (8) possesses a unique real solution. After that, by means of (3a), the temperatures T_2 and T_1 can be calculated. Finally, to determine the gas temperature in all internal points in the active discharge medium, expression (2) can be written in the form

$$T_{\rm g}(r) = \left[T_1^{m+1} + \frac{q_{\rm v}(m+1)}{4\lambda_0}\left(R_1^2 - r^2\right)\right]^{1/(m+1)}. \tag{9}$$

2.2 Determination of the heat transfer coefficient α and the gas temperature $T_{\rm g}$ at forced convection

In some cases, depending on the exploitation conditions, forced cooling of the laser tube with a directed air flow is required. In this case, we do not know of a possible method for determining the temperature profile in the tube cross section. To solve equation (1) with boundary conditions (3a) – (3b), we should find a dependence between the value α and new cooling conditions.

In the case of forced convection, criterion (5) is replaced by the Reinolds criterion [11]

$$\mathrm{Re} = \upsilon H/\nu\,. \tag{10}$$

Here, υ is the flow speed; H is a characteristic dimension of the tube. In the case of cross cooling, $H = d_3$.

For horizontal tubes with forced air cooling, we have [11]:

$$\mathrm{Nu} = 0.615\mathrm{Re}^{0.466}. \tag{11}$$

In this way, from (4), (10) and (11), α is represented by

$$\alpha = 0.615\,\frac{\lambda_{\rm air}}{d_3}\left(\frac{\upsilon d_3}{\nu_{\rm air}}\right)^{0.466}. \tag{12}$$

Boundary condition (3b) takes the form

$$q_l = 0.615\pi\lambda_{\rm air}\left(\frac{\upsilon d_3}{\nu_{\rm air}}\right)^{0.466}(T_3 - T_0) + \pi d_3\varepsilon c\left[\left(\frac{T_3}{100}\right)^4 - \left(\frac{T_0}{100}\right)^4\right]. \tag{13}$$

Equation (13) allows T_3 to be calculated. Then, as in the previous case, by using (3a) and (9) the temperature profile in the gas cross section can be determined.

3. Results and discussion

The data presented in Table 1 were used to calculate the temperature profile in the case of natural and forced convection.

3.1 Natural convection

The temperature distribution in the tube cross section is shown by curve (*1*) (Fig. 2). The calculated values derived by solving (8), (3a) and (9) are as follows: $T_3 = 617$ K, $T_2 = 1010$ K, $T_1 = 1020$ K and $T(0) = T_{\max} = 1967$ K.

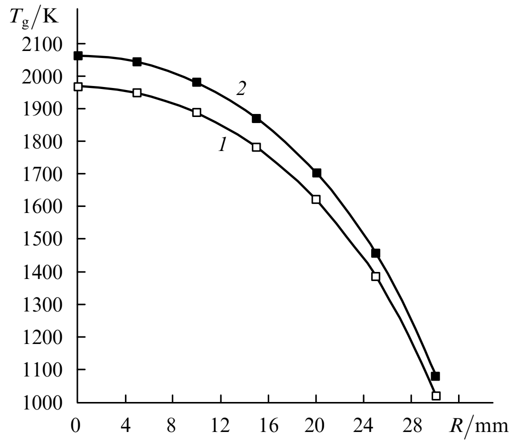

Figure 2. Gas temperature distribution in the cross section of the laser medium at natural convection: (*1*) – at power $Q = 4080$ W and (*2*) – at power $Q = 4488$ W.

In Fig. 3 the temperature distributions $T_{\rm q}(r)$ in the quartz wall and $T_{\rm i}(r)$ in the insulation are illustrated. They satisfy

$$T_{\rm q}(r) = T_1 - (T_1 - T_2)\,\frac{\ln(r/r_1)}{\ln(r_2/r_1)},$$

and

$$T_{\rm i}(r) = T_2 - (T_2 - T_3)\,\frac{\ln(r/r_2)}{\ln(r_3/r_2)}$$

(see [11]).

The method used until now in the literature required the knowledge of the temperature T_2 of the outer wall of the quartz tube, which can be measured if needed (for instance with a thermocouple). After that, assuming that $T_2 = T_1$ by

Table 1. Data used for calculating the temperature profile.

Q/W	$l_{\rm a}$/m	$q_{\rm v}$/W cm^{-3}	q_l/W m^{-1}	$\lambda_{\rm g} = \lambda_0 T^m$/W m^{-1} K^{-1}	λ_1/W m^{-1} K^{-1}	λ_2/W m^{-1} K^{-1}	ε
4080 [7, 8]	2 [7]	0.7219	2040	$\lambda_0 = 5.8935\times10^{-5}$ ($m = 1.091$, $p_{\rm Ne} = 15$ Torr, $p_{\rm H_2} = 0.3$ Torr) [10]	1.96 ($T = 800 - 1100$ K) [12]	0.12 ($T = 800 - 1100$ K, mineral insulation) [11]	0.72 [12]

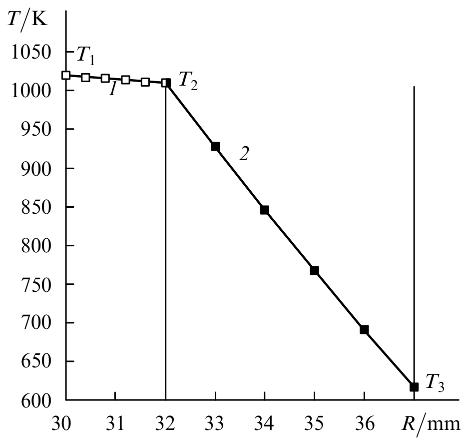

Figure 3. Temperature profile obtained in the quartz wall (*1*) and in the thermal insulation (*2*) at power $Q = 4080$ W.

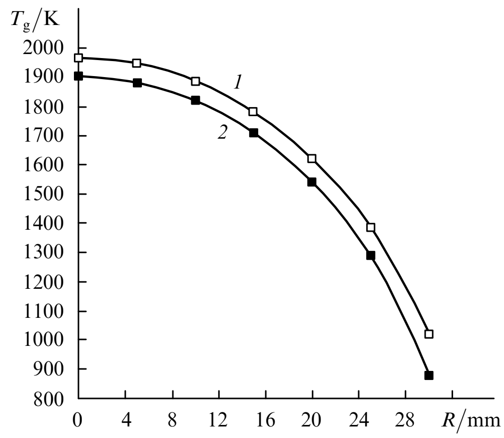

Figure 4. Gas temperature distribution in the cross section of the laser medium at natural convection for the power $Q = 4080$ W (*1*) and forced convestion for the power $Q = 4080$ W and flow velocity $\upsilon = 20$ m s^{-1}(*2*).

(2), the temperature in the laser tube is calculated (see [3, 7]). Our calculations show that the absolute error in this case is $\Delta T = T_1 - T_2 = 10$ K. The difference in temperatures is extremely small and such an assumption is applicable in reality.

The proposed method allows preliminary evaluation of the possible change in temperature in the case of a change in the input electric power. For example, by increasing the electric power by 10 %, the maximum temperature $T_{\max}$ raises by 96 °C [see Fig. 2, curve (*2*)]. Such preliminary calculations are not possible in the literature mentioned above because the temperature T_2 remains unknown.

At a known temperature T_3 equation (8) allows analysing the type of the heat transfer between the laser tube and the surroundings. In this case, the dominant heat transfer mechanism is the heat radiation, the contribution of which is 64 %, and the second one is the heat convection, the contribution of which is only 36 %.

3.2 Forced convection

When the laser source overheats during the exploitation process in some cases forced cooling is required – with a radially directed air flow, for example. As follows from section 2.2, we solve consecutively equations (13), (3a) and (9). The obtained results for the temperature profile during forced convection with air flow speed $\upsilon = 20$ m s^{-1} are illustrated in Fig. 4. The values of the temperatures at specific points are: $T_3 = 466$ K, $T_2 = 858$ K, $T_1 = 881$ K, $T(0) = T_{\max} = 1903$ K. By comparing these temperatures with the corresponding ones from the case of natural convection it becomes clear that the biggest discrepancy is obserbed for T_3: $\Delta T_3 = T_3^{\rm nat} - T_3^{\rm forc} = 617$ K $-$ 466 K $=$ 151 *K*, while the smallest one – for $T_{\max}$: $\Delta T_{\max} = T_{\max}^{\rm nat} - T_{\max}^{\rm forc} = 1967$ K $-$ 1903 K $=$ 64 K. Under conditions of forced convection the radial temperature gradient increases: $\Delta T_{\rm r}^{\rm nat} = T_{\max}^{\rm nat} - T_1^{\rm nat} = 1967$ K $-$ 1020 K $=$ 947 K, $\Delta T_{\rm r}^{\rm forc} = T_{\max}^{\rm forc} - T_1^{\rm forc} = 1903$ K $-$ 466 K $=$ 1437 K. The presence of a larger radial temperature gradient has a disadvantageous reaction on the laser power and the mode composition of the laser beam deteriorates.

The suggested method allows carrying out some computer simulations. For example, let us assume that the temperature profile [curve (*1*)] in Fig. 4 is optimal and gives the needed temperature comfort to the laser tube. This means that under conditions of forced convection we can increase the input electric power within certain limits until the initial temperature is achieved [in Fig. 4 the power can be increased until curve (*1*) and curve (*2*) match]. In this way, the laser generation can be increased without thermal overheating of the tube. It seems that by increasing the electric power, curve (*2*) cannot entirely match curve (*1*). In Fig. 5 curve (*1*) is constructed in such a way that there is a coincidence only with the maximum temperature $T_{\max} = 1967$ K. Such an approach is acceptable, because it will guarantee the thermal stability in the central part of the tube, where the active zone of the laser generation is located. In practice this realization is impossible, because in most cases the maximum temperature is unknown and there is a missing real physical indicator, which is supposed to show when we must stop increasing the electric power. This is why the electric power could be increased to equalise with $T_1 = 1020$ K – a value, which can be tracked by using a thermocouple. This is shown by curve (*3*) in Fig. 5. The calculations show that the maximum temperature increases by approximately 213 °C, but this could have a negative

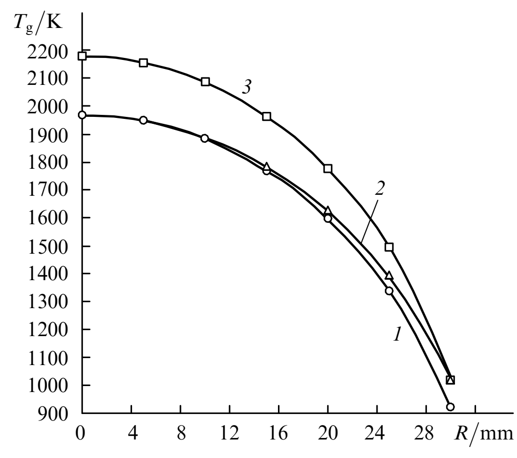

Figure 5. Temperature profile obtained in the laser tube: (*1*) – at forced convection, flow velocity $\upsilon = 20$ m s^{-1}, and $Q = 4360$ W; (*2*) – at natural convection, $Q = 4080$ W; (*3*) – at forced convection, flow velocity $\upsilon = 20$ m s^{-1} and $Q = 5310$ W.

effect on the thermal stability of the laser tube in the considered case.

4. Conclusions

A new approach for solving the heat conduction equation for a copper bromide vapour laser has been proposed. Based on mixed boundary conditions, which describe the heat interaction between the laser tube and the surroundings, the temperature profile in the active medium cross section is calculated. Two cases of cooling have been investigated – natural and forced convection. It is estimated that the main mechanism of the heat transfer process at natural convection is the heat radiation. The developed method allows preliminary evaluation of the gas temperature in computer simulations – a change in the geometrical design, the laser tube material and heat insulation, the input electric power, and exploitation conditions. A specific study of the temperature profile has been performed under the conditions of forced cooling. It has been established that in all the considered cases the radial temperature gradient of the medium increases.

Independent of the specific object of study the proposed method is easily adaptable and can be applied to a wide range of gas lasers, metal vapour lasers and metal compound vapour lasers.

Acknowledgements. This work was supported by the NSF of the Bulgarian Ministry of Education and Science (Project VU-MI-205/2006) and NPD of Plovdiv University 'Paisii Hilendarski' (Project 07M07).

References

1. Shiyanov D.V., Sukhanov V.B., Evtushenko G.S., Andrienko O.S. *Kvantovaya Elektron.*, **34**, 625 (2004) [*Quantum Electron.*, **34**, 625 (2004)].
2. Shiyanov D.V., Evtushenko G.S., Sukhanov V.B., Fedorov V.F. *Kvantovaya Elektron.*, **37**, 49 (2007) [*Quantum Electron.*, **37**, 49 (2007)].
3. Carman R.G., Brown D.J.W., Piper A. *IEEE J. Quantum Electron.*, **30**, 1876 (1994).
4. Yakovlenko S.I. *Kvantovaya Elektron.*, **30**, 501 (2000) [*Quantum Electron.*, **30**, 501 (2000)].
5. Boichenko A.M., Evtushenko G.S., Zhdaneev O.V., Yakovlenko S.I. *Kvantovaya Elektron.*, **33**, 1047 (2003) [*Quantum Electron.*, **33**, 1047 (2003)].
6. Petrash G.G. *Kvantovaya Elektron.*, **35**, 576 (2005) [*Quantum Electron.*, **35**, 576 (2005)].
7. Astadjov D.N., Dimitrov K.D., Jones D.R., Kirkov V.K., Little C.E., Sabotinov N.V., Vuchkov N.K. *IEEE J. Quantum Electron.*, **33**, 705 (1997).
8. Astadjov D.N., Sabotinov N.V. *J. Phys. D: Appl. Phys.*, **30**, 1507 (1997).
9. Kushner M.J., Warner B.E. *J. Appl. Phys.*, **54**, 2970 (1983).
10. Astadjov D.N., Vuchkov N.K., Sabotinov N.V. *IEEE J. Quantum Electron.*, **24**, 1926 (1988).
11. Oprev M., Batov S.G., Uzunov D.Z. *Toplotehnika* (Heat Technology) (Sofia: Technika, 1978).
12. Grigor'ev I.S., Meilikhov E.Z. (Eds) *Fizicheskie velichiny. Spravochnik* (Handbook of Physical Quantities) (Moscow: Energotomizdat, 1991).